

Team21 Final Report

B10401006 洪愷希, B10401008 李彥佑, B10902138 陳德維

June 5, 2024

Paper Title

Order Space-Based Morphology for Color Image Processing.

Abstract

Mathematical morphology is a fundamental tool based on order statistics for image processing, while binary and grayscale images, whose pixels can be sorted by their pixel values, i.e., each pixel has a single number. On the other hand, each pixel in a color image has three numbers corresponding to three color channels; therefore, it is difficult to sort color pixels uniquely. This paper proposed a method for unifying the orders of pixels sorted in each color channel separately, where we consider that a pixel exists in a three-dimensional space called order space, and derive a single order by a monotonically non-decreasing function defined on the order space. The proposed method treats three orders of pixels sorted in respective color channels equally. Therefore, the proposed method is consistent with the conventional morphological operations for binary and gray-scale images.

Motivation

For the first-half of the semester, we focus on image processing for single-channel(gray-scale) images only, and for RGB images, we tend to split them into 3 individual channel and process them respectively. However, despite it make sense to handle each channel individually, we are curious that whether it is possible to have a end-to-end method to process RGB images. Hence we want to extend morphological processing from gray-scale images to RGB images.

Problem Definition

Given n pixels f_1, f_2, \dots, f_n , each with R, G, B values. Find the order O_1, O_2, \dots, O_n of the pixels, where O_i is the order of f_i among all pixels.

Introduction

Mathematical morphology is a theory that originated in the 1960s for treating the shape of objects in images based on set theory and lattice theory. Mathematical morphology has a wide range of applications in digital image processing, where the development of basic techniques for binary and gray-scale images is almost complete. However, mathematical morphology for color images and higher-dimensional images is still under study because of the difficulty and uncertainty of ordering vector data, such as color vectors or pixels,

in color images.

This paper proposed a method for morphologically operating color images on the basis of an order space, which is a three-dimensional space with the axes of orders of pixels in three color channels. Specifically, they take the RGB color channels as a typical example, and sort the pixels in each channel separately. As a result, they obtain a triplet of orders for each pixel, which is then represented as a point in the order space. After that, they compute a single order from the obtained triplet of orders by a function from 3D to 1D, and then apply morphological operations based on the single order of pixels.

Algorithm

Algorithm 1: Mapping from RGB color space to order space

Data: a set of pixels $\{f_{i+k,j+l} = [f_{i+k,j+l}^R, f_{i+k,j+l}^G, f_{i+k,j+l}^B] \mid (k, l) \in S\}$ (S is the structuring element used in operation)

Result: a set of coordinates in order space $\{(o_\xi^R, o_\xi^G, o_\xi^B) \mid \xi \in \{1, 2, \dots, |S|\}\}$

```

1 Assign serial numbers  $\xi \in \{1, 2, \dots, |S|\}$  to all pixels in the required set to have a
   set of re-indexed pixels  $\{f_\xi = [f_\xi^R, f_\xi^G, f_\xi^B] \mid \xi \in \{1, 2, \dots, |S|\}\}.$ 
2 for  $X \in \{R, G, B\}$  do
3    $[a_1^X, a_2^X, \dots, a_{|S|}^X] = argsort(f_1^X, f_2^X, \dots, f_{|S|}^X);$ 
4   for  $\xi \in \{1, 2, \dots, |S|\}$  do
5      $o_{a_\xi^X}^X = \xi;$ 
6   end
7 end
8 return  $\{(o_\xi^R, o_\xi^G, o_\xi^B) \mid \xi \in \{1, 2, \dots, |S|\}\}$ 

```

Order Space-Based Morphology for Color Image Processing

Let $F = [f_{ij}]$ be an RGB color image, where $f_{ij} = [f_{ij}^R, f_{ij}^G, f_{ij}^B]$ denotes the RGB color vector at the position (i, j) in F .

Then, we can sort the color components covered by a structuring element in ascending order of their values, e.g., $f_{i+k(a_1^R), j+l(a_1^R)}^R \leq f_{i+k(a_2^R), j+l(a_2^R)}^R \leq \dots \leq f_{i+k(a_5^R), j+l(a_5^R)}^R$ for the R component with a structuring element S with five pixels, where $a_1^R, a_2^R, \dots, a_5^R$ denote the sorted indices of pixels covered by S , and $k(a_i^R)$ and $l(a_i^R)$ denote the vertical and horizontal relative coordinates of the pixel corresponding to a_i^R , respectively.

Let $\xi = a_\eta^R$ (for $\eta = 1, 2, \dots, 5$) be a function where a pixel index ξ is related to an order

η given by the above sorting procedure. Then, we consider the inverse function of $\xi = a_\eta^R$ as $\eta = o_\xi^R = (a^R)_\xi^{-1}$. Similarly, we can sort the G components and B components and consider the inverse function to get o_ξ^G and o_ξ^B .

In the 3D order space, an RGB color pixel with an index ξ is represented by a triplet $(o_\xi^R, o_\xi^G, o_\xi^B)$. To define dilation and erosion for an RGB color image, we need to reduce the triplet $(o_\xi^R, o_\xi^G, o_\xi^B)$ to a singlet o_ξ . There are some equations to achieve this:

$$o_\xi^S = o_\xi^R + o_\xi^G + o_\xi^B$$

$$o_\xi^P = o_\xi^R o_\xi^G o_\xi^B$$

$$o_\xi^M = \text{median}(o_\xi^R, o_\xi^G, o_\xi^B)$$

Once we reduce $(o_\xi^R, o_\xi^G, o_\xi^B)$ to o_ξ , we can define the dilation and erosion of F by S as follows:

$$D(F, S) = [d_{ij}], d_{ij} = f_{\xi^{max}} \quad \xi^{max} = \arg \max_{\xi \in \{1, 2, \dots, |S|\}} o_\xi$$

$$E(F, S) = [e_{ij}], e_{ij} = f_{\xi^{min}} \quad \xi^{min} = \arg \min_{\xi \in \{1, 2, \dots, |S|\}} o_\xi$$

Also, we can combine the above dilation and erosion operations for defining opening and closing operations as follows:

$$O(F, S) = D(E(F, S), S)$$

$$C(F, S) = E(D(F, S), S)$$

Combining the above opening and closing operations, we can define open–closing and close–opening operations as follows:

$$OC(F, S) = C(O(F, S), S)$$

$$CO(F, S) = O(C(F, S), S)$$

Fuzzy Morphological Operations by Exponentially Weighted Averaging

We extend the previous order space-based morphological operations, which are crisp operations, to fuzzy ones by introducing an exponentially weighted averaging method.

Assume that an order o_ξ for $\xi \in 1, 2, \dots, |S|$ is obtained from a set of triplets $(o_\xi^R, o_\xi^G, o_\xi^B)$. Then, we define a fuzzy dilation by introducing an exponentially weighted averaging as

follows:

$$D^{FUZ}(F, S, \alpha) = [d_{ij}^{FUZ}], \quad d_{ij} = \frac{\sum_{\xi=1}^{|S|} \exp(\alpha o_\xi) f_\xi}{\sum_{\xi=1}^{|S|} \exp(\alpha o_\xi)},$$

where \exp denotes the exponential function defined by $\exp(x) = e^x$, where e is a constant called Euler's number and α is a positive constant for controlling the fuzziness.

Similarly, we can define a fuzzy erosion as follows:

$$E^{FUZ}(F, S, \alpha) = [e_{ij}^{FUZ}], \quad e_{ij} = \frac{\sum_{\xi=1}^{|S|} \exp(-\alpha o_\xi) f_\xi}{\sum_{\xi=1}^{|S|} \exp(-\alpha o_\xi)},$$

Combining these operations, we have fuzzy opening and closing operations as follows:

$$O^{FUZ}(F, S, \alpha) = D^{FUZ}(E^{FUZ}(F, S, \alpha), S, \alpha)$$

$$C^{FUZ}(F, S, \alpha) = E^{FUZ}(D^{FUZ}(F, S, \alpha), S, \alpha)$$

From these, we further define fuzzy open-closing and close-opening operations as follows:

$$OC^{FUZ}(F, S, \alpha) = C^{FUZ}(O^{FUZ}(F, S, \alpha), S, \alpha)$$

$$CO^{FUZ}(F, S, \alpha) = O^{FUZ}(C^{FUZ}(F, S, \alpha), S, \alpha)$$

Expected Experimental Result

Figure 1 is a noisy input image including 10% impulse noise, where 6553 out of $256 \times 256 = 65,536$ pixels are corrupted with impulse noise for evaluation compared with Wang's hypergraph-based method (Wang, J.; Liang, G.; Wu, Y.; Li, Y.; Hu, J. New colour morphological operators on hypergraph. *IET Image Process.* **2018**, 12, 690–695.)



Figure 1

Wang's method has two parameters, μ and β , which are set as $\mu = 250$ and $\beta = 1$ by adjusting for this noise removal task through preliminary experiments. The proposed method with 'Cross' and 'Square' structuring elements shown in **Figure 2a** and **Figure 2b**, respectively.

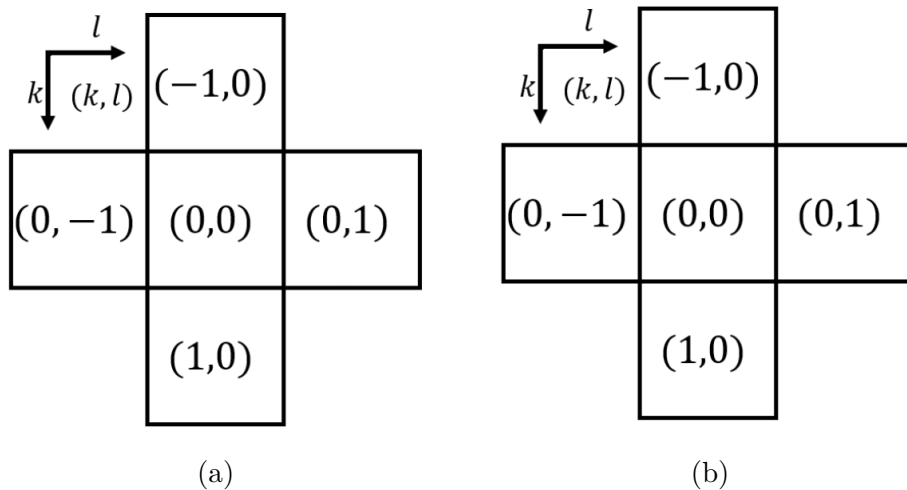


Figure 2

Below are the noise removal results using Wang's method (**top** row) and the proposed order space-based morphological operations (**middle** and **bottom** rows) with o^S for a noisy image in **Figure 1**, where their subcaptions denote the ‘operation/structuring element’ used for computing respective images: The top row shows the results of Wang's method, where ‘HG’ indicates that the structuring elements are given by hypergraphs. The middle and bottom rows show the results of the proposed method with ‘Cross’ and ‘Square’ structuring elements shown in **Figure 2**. The six columns from left to right show the results of dilation (Dilat.), erosion (Eros.), opening (Open.), closing (Clos.), open-

closing (O.-c.) and close-opening (C.-o.) operations, respectively.



Figure 3

Table 1 shows the values of the peak signal-to-noise ratio (PSNR) [25] between the output images in **Figure 1**

Table 1: PSNR for output images in **Figure 1**

SE	Dilation	Erosion	Opening	Closing	Open-Closing	Close-Opening
'HG'	15.31	16.22	20.11	20.52	20.88	21.59
'Cross'	18.82	18.80	22.96	23.11	25.14	25.13
'Square'	17.79	17.73	23.67	23.97	25.74	25.83

The performance of noise removal is evaluated by the mean PSNR among the 12 different images as summarized in **Figure 4**, where **Figure 4a**, **4b** show the results of open-closing and close-opening, respectively. In each graph, the vertical and horizontal axes denote the mean PSNR among the 12 images and the density of impulse noise varying from 10% to 60%, respectively, and the line colors, blue, orange, green and red correspond to Wang's method and the proposed methods with o^S , o^P and o^M , respectively. In both graphs, Wang's method (blue line) obtains higher values of mean PSNR than the proposed methods with o^P and o^M (green and red lines), and the proposed method with o^S (orange line) outperforms Wang's method.

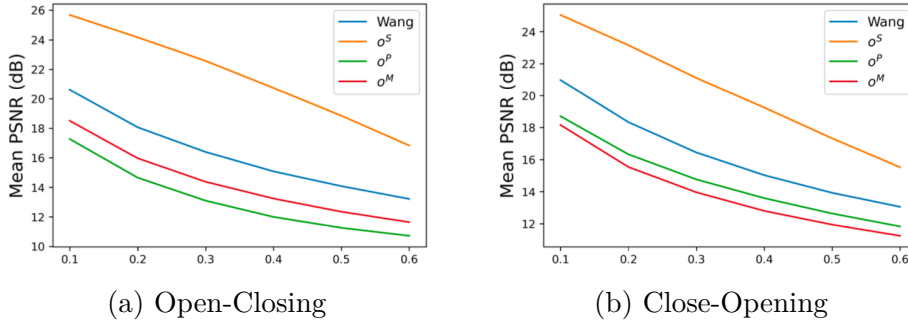


Figure 4

They also compared the performance of grayscale and color morphological operations as illustrated in **Figure 5**, where a color original image (top left box) is corrupted by Gaussian or impulsive noise to produce a noisy image (top right box).

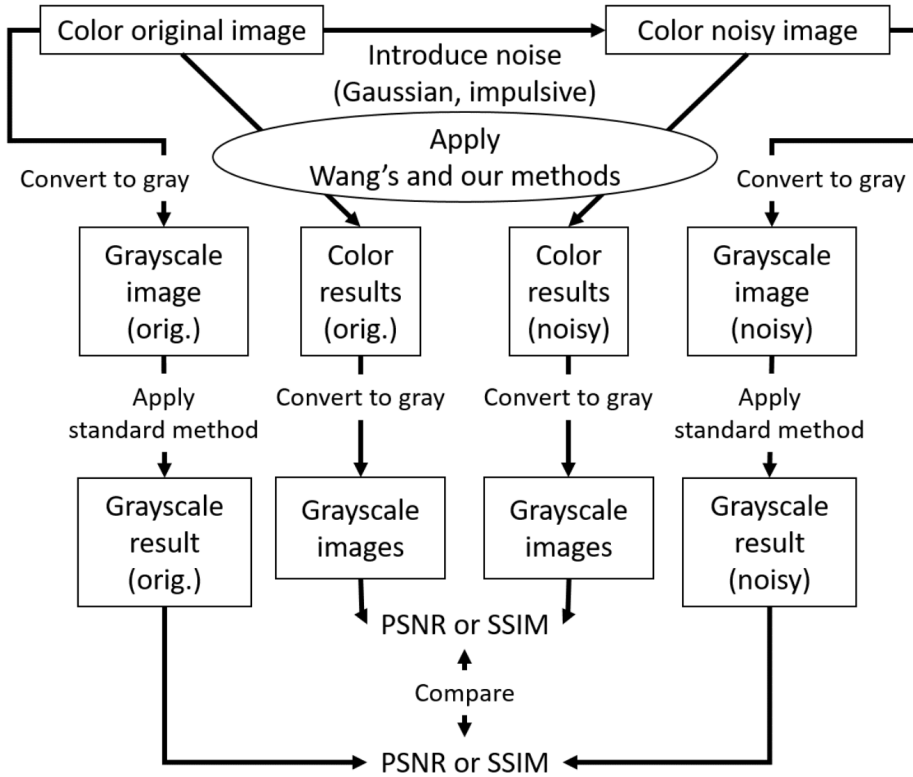


Figure 5

Figure 6 shows the results of **Gaussian noise** removal with the SIDBA dataset, where the vertical axes denote **Figure 6a** PSNR and **Figure 6b** SSIM, and the horizontal axes denote the compared methods. In this figure, the grayscale operation achieved the highest PSNR and SSIM values, and the proposed method outperformed Wang's method.

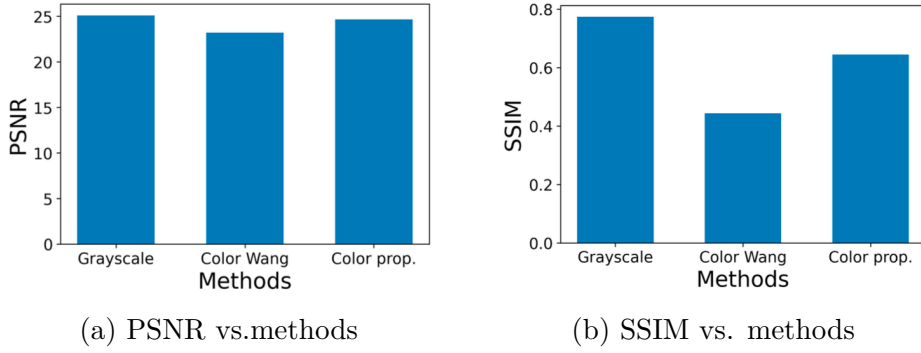


Figure 6: Results of Gaussian noise removal

Figure 7 shows the results of impulse noise removal, where the settings of axes are the same as **Figure 6**. In **Figure 7a**, the proposed method achieved the highest PSNR value, while in **Figure 7b**, the grayscale operation achieved the highest SSIM value. The reason why the grayscale operation achieves higher values than color ones is speculated to be that the conversion from color to gray has a noise-reduction effect.

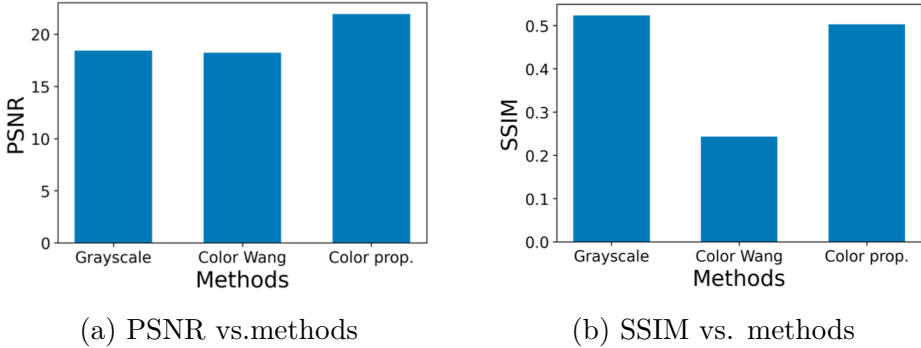


Figure 7: Results of impulse noise removal

The above speculation is investigated in **Table 2**, where color noisy images are compared with grayscale noisy images by PSNR and SSIM for Gaussian and impulse noises. The values of the image quality measure for R, G and B components are improved by grayscale conversion for all combinations of noises and measures. This result shows that the grayscale conversion has a noise-reduction effect. In terms of the color morphological operations in this experiment, the proposed method achieved better PSNR and SSIM values than Wang's method.

Table 2: Comparison of the quality of noisy images between color and gray

Noise	Quality Measure	R	G	B	Gray
Gaussian	PSNR	18.90	19.06	19.03	22.71
Gaussian	SSIM	0.306	0.350	0.315	0.417
Impulse	PSNR	12.16	11.94	12.01	16.63
Impulse	SSIM	0.118	0.144	0.122	0.183

Next, they show the experimental results for the fuzzy morphological operations. **Figure 8** shows the PSNR values for different values of α varying from 0.1 to 1.0, where we applied the fuzzy open–closing to the noisy image in **Figure 1**. We observe that $\alpha = 0.5$ achieves the highest PSNR value, and use $\alpha = 0.5$ below.

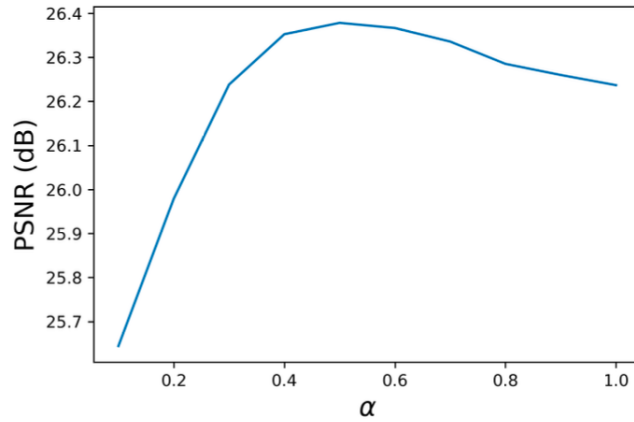


Figure 8

Figure 9 shows the results of the proposed fuzzy morphological operations. The order of the output images (a–f) by six morphological operations, dilation (Dilat.), erosion (Eros.), opening (Open.), closing (Clos.), open–closing (O.-c.) and close–opening (C.-o.).



Figure 9

Figure 10 shows the effectiveness quantitatively by comparing the mean PSNR values computed with the SIDBA dataset between crisp and fuzzy operations, where the vertical and horizontal axes denote the mean PSNR and noise density as well as the settings from **Figure 4**, and **Figure 10a,b** which show the results of open–closing and close–opening

operations, respectively. For both operations, the fuzzy ones denoted by purple lines outperform the crisp ones denoted by orange lines.

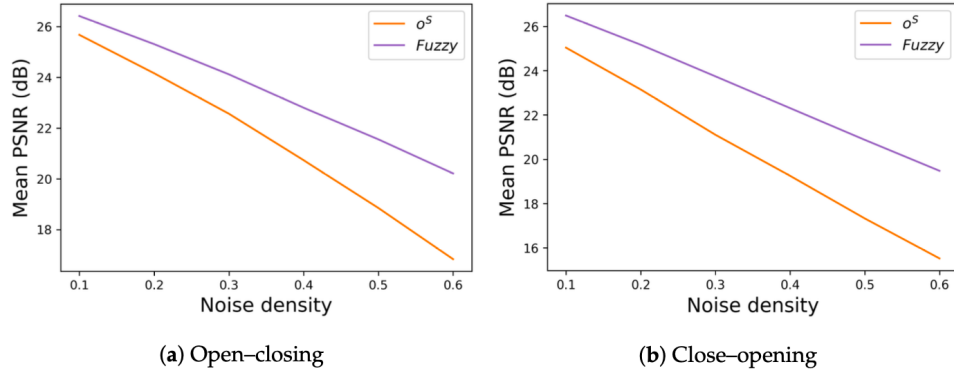


Figure 10

Discussion and Conclusion

- The proposed method is a method by which the obtained three orders, which form a 3D order space, can be unified into a single order of pixels in a suitable manner for a given application.
- The ways of unifying three orders are not restricted to the three methods presented in this paper. Investigating better ways to unify plural orders into one will be a promising future research direction.
- Extended the proposed order space-based morphological operations to their fuzzy version, where we proposed a method for fuzzifying morphological operations by exponentially weighted averaging.
- The noise removal performance was further improved by the fuzzification for both open-closing and close-opening operations, both of which achieved better performance than dilation, erosion, opening and closing operations in a conventional crisp situation.
- Future work will include the extension of the proposed method for color image processing to multidimensional data processing, which will also be fuzzified by the proposed exponentially weighted averaging method to improve the performance.

Our Result

原始圖片：



Basic Operations

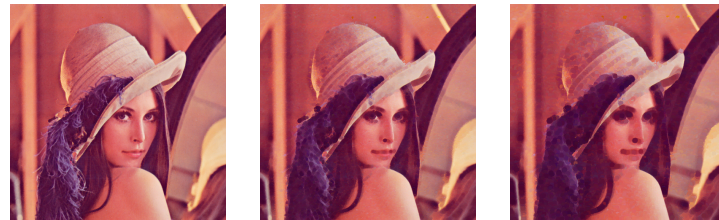
下圖比較我們實作後由不同模式進行 morphological operations 的結果。以視覺上而言



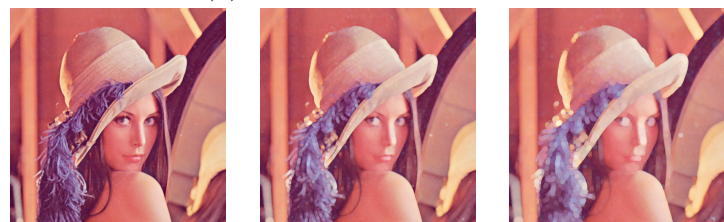
Figure 11: Comparison of different modes

並無明顯差異，和論文一致。

接著比較使用不同大小的 structuring element 進行 morphological operations 的結果。可看出，隨著 structuring element size 的增加，圖片的變化也越來越明顯。



(a) erosion with different SE



(b) dilation with different SE

Figure 12: morphological operations with different structuring element size

我們也嘗試了另一種 ordering 的方法作為參照：先將圖片轉為 HSV，接著以 (V, S, H) 的順位進行比較。此外也附上轉為灰階後 morphological operations 的結果。



Figure 13: Comparison of RGB and HSV orderings

大致效果相似，不過放大觀察可以看出本論文使用的方法在不同顏色交界上最為平滑且保留細節。

Denoising

首先，我們在圖片中分別加入 10% 的 salt 及 pepper noise，並分別使用 opening 及 closing 進行 denoising。

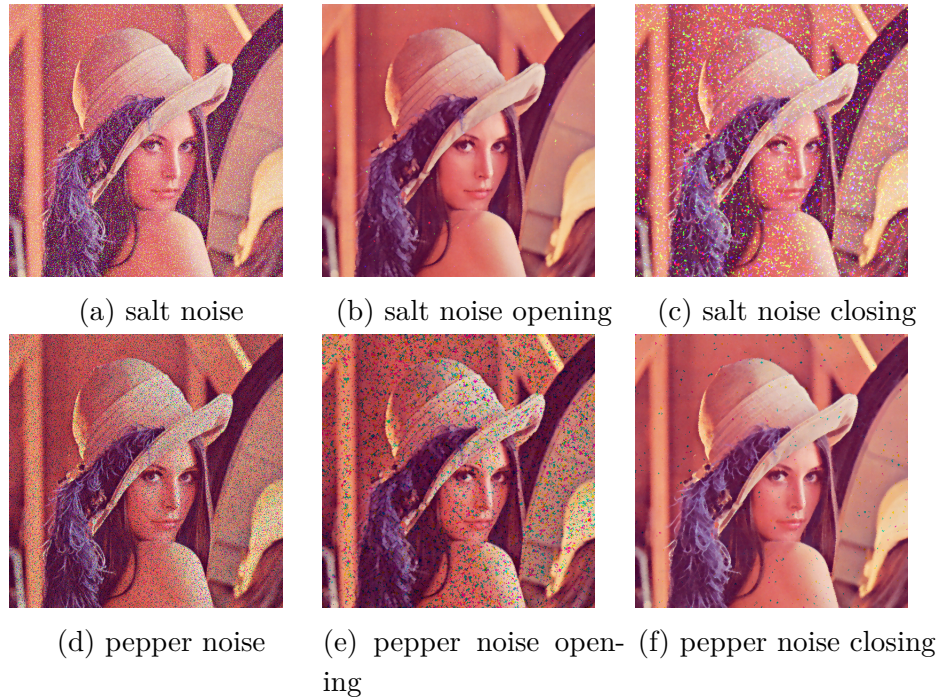
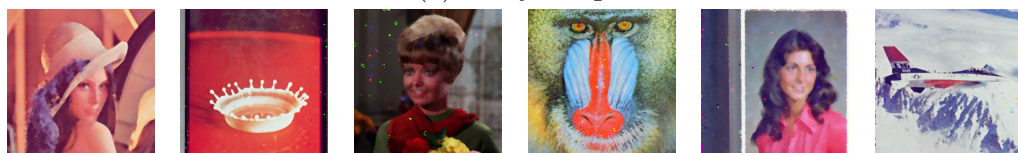


Figure 14: pepper/salt noise

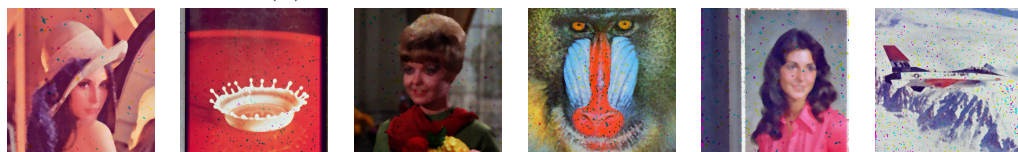
接著我們在許多圖片加入 10% impulse noise，並比較 open-closing，close-opening 以及 Wang 等人所提出的 hypergraph 方法 [2]。Wang 的部分為我們參考其原始論文並實作而來。



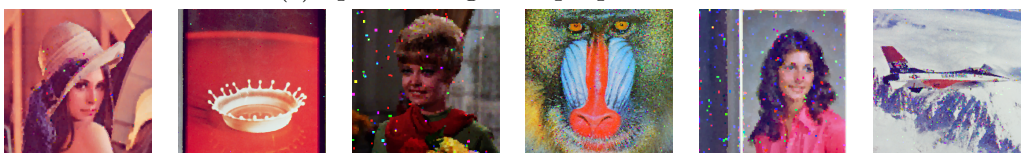
(a) Noisy images



(b) close-opening with proposed method



(c) open-closing with proposed method



(d) Wang's close-opening

denoising with impulse noise

Our Discussion

The evil argsort

這是我們在實作中遇到比較大的問題：`argsort` 遇到相同值應如何處理。這個問題並沒有在文中提及，而以 numpy 的實作來看，`argsort` 會回傳最早出現的 index。不過這卻會導致嚴重的問題，例如有以下的 pixels：

$$p_1 = (0, 0, 0)$$

$$p_2 = (0, 0, 0)$$

$$p_3 = (0, 0, 0)$$

$$p_4 = (255, 0, 0)$$

顯然，我們預期 p_4 的 order 最大。然而，使用 `np.argsort` 所產生的 order 如下：

$$\begin{aligned} p_1 &= (2, 3, 3) \\ p_2 &= (1, 2, 2) \\ p_3 &= (0, 1, 1) \\ p_4 &= (3, 0, 0) \end{aligned}$$

若選擇 `sum` 作為 reducing function，則最後的 order 為：

$$\begin{aligned} p_1 &= 8 \\ p_2 &= 5 \\ p_3 &= 2 \\ p_4 &= 3 \end{aligned}$$

這並不是一個合理的結果。因此，比較理想的做法是改定義 order 為「所有 pixels 中小於此 pixel 的個數」，才能避免前述的問題。在下一節的圖片中我們將呈現這個問題。

Global vs. Local

除了前一節的問題以外，我們也發現 order 可以用兩種方式來計算：

- Global order：將整張圖片的所有 pixels 一起排序。
- Local order：針對每個 pixel，只考慮將 structuring element 放在此 pixel 時所涵蓋的 pixels。

最終我們發現使用 local order 才能實作出論文中的效果。下圖我們呈現這兩節所提到的 pitfalls，以及實作成功的版本作為比較。



(a) Local orders



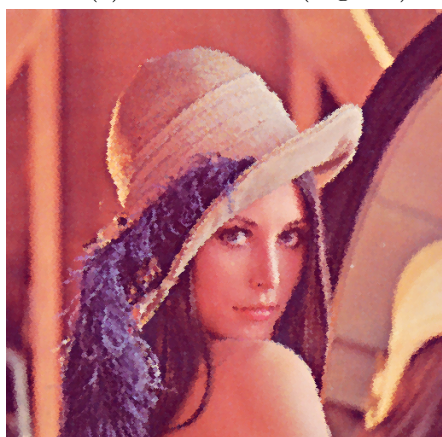
(b) Local orders (fuzzy)



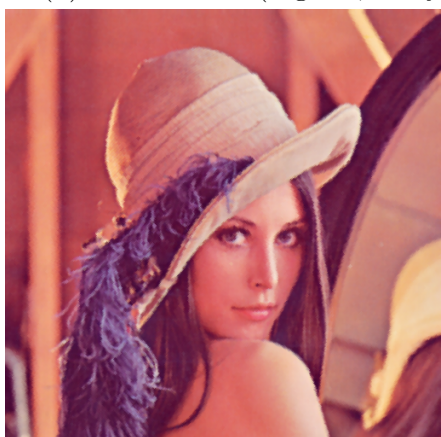
(c) Local orders (argsort)



(d) Local orders (argsort, fuzzy)



(e) Global orders



(f) Global orders (fuzzy)

Figure 16: Comparison of dilation with global and local orders

Referenced Paper

- [1] Sun, S.; Huang, Y.; Inoue, K.; Hara, K. Order Space-Based Morphology for Color Image Processing. *J. Imaging* **2023**, 9, 139. <https://doi.org/10.3390/jimaging9070139> [2] Wang, J., Liang, G., Wu, Y., Li, Y., Hu, J. (2018). New colour morphological operators on hypergraph. In IET Image Processing (Vol. 12, Issue 5, pp. 690–695). *Institution of Engineering and Technology (IET)*. <https://doi.org/10.1049/iet-ipr.2017.0468>

Division of the work

- B10401006 洪愷希
 - Implementation Code
 - *Out Result, Our Discussion Section*
- B10401008 李彥佑
 - Math & Algorithm parts of report
 - Wang's Method Implementation
- B10902138 陳德維
 - Dataset Preparation
 - Proposal & Final Report